

Requirement of FAT and DCHS protocadherins during hypothalamic-pituitary development

Emily J. Lodge, ... , Constantine Stratakis, Cynthia L. Andoniadou

JCI Insight. 2020. <https://doi.org/10.1172/jci.insight.134310>.

Research In-Press Preview Development Endocrinology

Pituitary developmental defects lead to partial or complete hormone deficiency and significant health problems. The majority of cases are sporadic and of unknown cause. We screened 28 patients with pituitary stalk interruption syndrome (PSIS) for mutations in the FAT/DCHS family of protocadherins that have high functional redundancy. We identified seven variants, four of which putatively damaging, in *FAT2* and *DCHS2* in six patients with pituitary developmental defects recruited through a cohort of patients with mostly ectopic posterior pituitary gland and/or pituitary stalk interruption. All patients had growth hormone deficiency and two presented with multiple hormone deficiencies and small glands. *FAT2* and *DCHS2* were strongly expressed in the mesenchyme surrounding the normal developing human pituitary. We analyzed *Dchs2*^{-/-} mouse mutants and identified anterior pituitary hypoplasia and partially penetrant infundibular defects. Overlapping infundibular abnormalities and distinct anterior pituitary morphogenesis defects were observed in *Fat4*^{-/-} and *Dchs1*^{-/-} mouse mutants but all animal models displayed normal commitment to the anterior pituitary cell type. Together our data implicate FAT/DCHS protocadherins in normal hypothalamic-pituitary development and identify *FAT2* and *DCHS2* as candidates underlying pituitary gland developmental defects such as ectopic pituitary gland and/or pituitary stalk interruption.

Find the latest version:

<https://jci.me/134310/pdf>



Requirement of FAT and DCHS protocadherins during hypothalamic-pituitary development

Emily J. Lodge^{1,*}, Paraskevi Xekouki^{1,2,*}, Tatiane S. Silva³, Cristiane Kochi³, Carlos A. Longui³, Fabio R. Faucz⁴, Alice Santambrogio^{1,5}, James L. Mills⁶, Nathan Pankratz⁷, John Lane⁷, Dominika Sosnowska¹, Tina Hodgson¹, Amanda L. Patist¹, Philippa Francis-West¹, Françoise Helmbacher⁸, Constantine A. Stratakis⁴, Cynthia L. Andoniadou^{1,5}

¹Centre for Craniofacial and Regenerative Biology, King's College London, Floor 27 Tower Wing, Guy's Campus, London, SE1 9RT, United Kingdom

²Current address: Endocrinology and Diabetes Clinic, University General Hospital of Heraklion, University of Crete Medical School, Heraklion Crete, 71003, Greece

³Pediatric Endocrinology Unit, Irmandade da Santa Casa de Misericórdia de São Paulo, São Paulo, Brazil.

⁴Section on Endocrinology and Genetics, Eunice Kennedy Shriver National Institute of Child Health and Human Development, National Institutes of Health (NIH), Bethesda, Maryland

⁵Department of Medicine III, University Hospital Carl Gustav Carus, Technische Universität Dresden, Dresden 01307, Germany

⁶Division of Intramural Population Health Research, Epidemiology Branch, Eunice Kennedy Shriver National Institute of Child Health and Human Development (NICHD), National Institutes of Health (NIH), Bethesda, Maryland, USA

⁷Department of Laboratory Medicine and Pathology, University of Minnesota Medical School, Minneapolis, Minnesota, USA

⁸Aix Marseille Université, CNRS, IBDM - UMR7288, Marseille, France.

* These authors contributed equally to this work

Correspondence: Cynthia L. Andoniadou

Address: Centre for Craniofacial and Regenerative Biology, King's College London, Floor 27 Tower Wing, Guy's Campus, London, SE1 9RT, United Kingdom

Tel +44 207 188 7389

Fax +44 207 188 1674

Email : cynthia.andoniadou@kcl.ac.uk

The authors have declared that no conflict of interest exists.

1 **Abstract**

2 Pituitary developmental defects lead to partial or complete hormone deficiency and
3 significant health problems. The majority of cases are sporadic and of unknown cause. We
4 screened 28 patients with pituitary stalk interruption syndrome (PSIS) for mutations in the
5 FAT/DCHS family of protocadherins that have high functional redundancy. We identified
6 seven variants, four of which putatively damaging, in *FAT2* and *DCHS2* in six patients with
7 pituitary developmental defects recruited through a cohort of patients with mostly ectopic
8 posterior pituitary gland and/or pituitary stalk interruption. All patients had growth
9 hormone deficiency and two presented with multiple hormone deficiencies and small
10 glands. *FAT2* and *DCHS2* were strongly expressed in the mesenchyme surrounding the
11 normal developing human pituitary. We analyzed *Dchs2*^{-/-} mouse mutants and identified
12 anterior pituitary hypoplasia and partially penetrant infundibular defects. Overlapping
13 infundibular abnormalities and distinct anterior pituitary morphogenesis defects were
14 observed in *Fat4*^{-/-} and *Dchs1*^{-/-} mouse mutants but all animal models displayed normal
15 commitment to the anterior pituitary cell type. Together our data implicate FAT/DCHS
16 protocadherins in normal hypothalamic-pituitary development and identify *FAT2* and *DCHS2*
17 as candidates underlying pituitary gland developmental defects such as ectopic pituitary
18 gland and/or pituitary stalk interruption.

19

20 **Introduction**

21 Developmental pituitary defects affect 0.5 in 100,000 live births and may lead to varying
22 degrees of pituitary hormone deficiency (1, 2). Beyond biochemical confirmation of
23 hormonal defects, diagnosis is based on magnetic resonance imaging (MRI) to identify a
24 small or absent anterior pituitary, interrupted or absent pituitary stalk (pituitary stalk
25 interruption syndrome or PSIS) and ectopic posterior pituitary (EPP) (3).

26 During embryonic development, a region of the ventral diencephalon of the
27 hypothalamus termed the infundibulum, and a region of the oral epithelium termed
28 Rathke's pouch (RP), evaginate towards each other to form the pituitary gland. These
29 actions are mediated by an array of developmental signals as well as the action of the
30 surrounding mesenchyme (for review see (4)). RP gives rise to the anterior pituitary whilst
31 the infundibulum gives rise to the posterior pituitary and the pituitary stalk, which connects
32 the posterior lobe to the hypothalamus. The vast majority of cases with pituitary
33 developmental defects are sporadic and of unknown cause; few cases appear to be familial
34 and they are often attributed to germline biallelic mutations in transcription factors
35 involved in the development of the infundibulum (5-7). Recently a whole exome sequencing
36 (WES) screen of patients with such defects identified compound defects in *DCHS1* among
37 other gene variants, indicating that protocadherins could be involved in pituitary
38 development (8).

39 Cadherins represent a major family of adhesion molecules involved in tissue
40 formation. As such they possess extracellular domains which facilitate binding, as well as an
41 intracellular domain capable of associating with adaptor and signaling proteins (9). FAT and
42 DCHS protocadherins act as ligand-receptor pairs when expressed in adjacent cells and have

43 been implicated both in planar cell polarity (PCP) regulating cell movements such as
44 convergence-extension and cell migration (10, 11), as well as regulation of YAP/TAZ
45 independently of the Hippo kinase cascade (12-14), which controls tissue proliferation and
46 stem cell activity (15).

47 In humans there are four *FAT* paralogues (*FAT1*, *FAT2*, *FAT3* and *FAT4*) and two *DCHS*
48 paralogues (*DCHS1* and *DCHS2*) (16). Mutations in *FAT4* are linked to Hennekam syndrome,
49 whilst biallelic mutations in *FAT4* or *DCHS1* genes are associated with Van Maldergem
50 syndrome (VMS). Besides symptoms common to both syndromes, such as intellectual
51 disability and craniofacial malformations, VMS-specific clinical symptoms additionally
52 include camptodactyly, syndactyly, small kidneys, osteopenia and tracheal abnormalities
53 (14, 17-21), whereas lymphangiectasia and lymphedema are specific to Hennekam
54 syndrome (17, 18, 22). A link between VMS and endocrine abnormalities including
55 hypogonadotropic hypogonadism and amazia, were reported in a recent study, providing
56 new support to the possible involvement of FAT/DCHS signaling in hypothalamic-pituitary
57 axis development or function (23). Null deletions of *Fat4* or *Dchs1* in mouse lead to
58 overlapping phenotypes, including inner ear, neural tube, kidney, skeleton, lung, and heart
59 defects (24) further supporting that these protocadherins act as a ligand-receptor pair.
60 However, both mutant mice die shortly after birth, inhibiting the study of postnatal
61 homozygous null animals (24, 25). *Dchs2*^{-/-} mutant mice are viable and fertile, with analyses
62 revealing functional redundancy between DCHS2 and DCHS1 (26). DCHS1 exhibits a broader
63 expression pattern during development and its loss generally results in more severe
64 developmental phenotypes (16). We have previously characterized expression patterns of
65 *Dchs1*, *Fat3* and *Fat4* during murine embryonic development and identified expression in
66 the hypothalamus, infundibulum, developing RP and surrounding mesenchyme (27).

67 In this study we performed WES on 28 patients with EPP and/or PSIS and identified
68 variants in *FAT2* and *DCHS2* predicted to be deleterious. We characterized expression of
69 *FAT2* and *DCHS2* in the human developing gland and analyzed pituitary development in a
70 series of *FAT/DCHS* mouse mutants (*Dchs1*, *Dchs2*, *Fat4*), which identified a range of
71 infundibular and RP defects. Our data suggest a requirement for *FAT* and *DCHS*
72 protocadherins in the infundibulum and mesenchyme surrounding the developing gland
73 during morphogenesis, revealing that *FAT/DCHS* function is necessary for normal pituitary
74 morphogenesis and their dysfunction can underlie developmental anomalies of the
75 hypothalamic-pituitary axis.

76

77 **Results**

78 **Molecular and *in silico* findings in patients with pituitary developmental defects**

79 Combined with our description of expression of *FAT/DCHS* family members during pituitary
80 development (27), the recent identification of links between *DCHS* abnormalities and
81 pituitary developmental defects (8, 23) suggested an involvement of *FAT/DCHS* signaling in
82 hypothalamic and/or pituitary development. To address this possibility, we studied 28
83 patients with congenital pituitary abnormalities of EPP and/or PSIS to whole exome
84 sequencing, focusing on all four *FAT* genes, as well as *DCHS1* and *DCHS2*. Three
85 heterozygous variants in *DCHS2* and four in *FAT2* were identified and their locations on the
86 proteins summarized in a schematic (Figure 1A). The variants, their functional type, class
87 (synonymous, non-synonymous, or frameshift), effect (missense, nonsense, silent),
88 frequency in control database and the genes in which these variants were identified in

89 patients with EPP are presented in Table 1. The allele frequency of all variants in the cohort
90 was 1.79%. Among all variants across these genes, only two variants in *DCHS2* and one
91 variant in *FAT2* were classified as functionally 'high' and predicted to be deleterious using
92 prediction tools (see Methods) (Table 1).

93 **Clinical Data**

94 The clinical and biochemical data of the six patients identified with *FAT2* and *DCHS2* variants
95 are summarized in Table 2. Patient D190 was a 20.6-year-old male at the time of
96 assessment, who was born full-term with cryptorchidism and micropenis. He was diagnosed
97 with multiple anterior pituitary hormone deficiencies and learning difficulties and received
98 full hormone replacement therapy. MRI showed EPP and a very small anterior pituitary for
99 his age and sex (Figure 1B). The patient required testosterone treatment for micropenis and
100 for pubertal induction and maintenance. Despite long-term follow-up, he never presented
101 any increment in testicular volume. He was found to harbor a *DCHS2* stop codon c.C4027T
102 (p.R1343*) variant (Table 1). This was also found in the atherosclerosis risk in communities
103 study (ARIC) controls and is reported as a rare variant in the gnomAD database and likely
104 deleterious based on the CADD prediction tool (Table 1).

105 Patient D041 was a 16.4-year-old male who was born full term. He developed growth
106 hormone deficiency (GHD) and was treated with recombinant growth hormone (rGH) until
107 the age of 16 years. His pituitary MRI revealed EPP and an anterior pituitary within the normal
108 size range for his age and sex (Figure 1B). Molecular analysis revealed a synonymous *FAT2*
109 variation F1497= (Table 1). This is reported as a very rare variant in the gnomAD database,
110 although it is predicted to be likely benign based on CADD score (Table 1).

111 Patient D965 was a 13.9-year-old male at the time of assessment who was born at 34 weeks
112 of gestation. He was diagnosed with GHD and MRI revealed an EPP (Table 2 and Figure 1B).
113 He was still under rGH treatment during clinical assessment. Molecular analysis revealed a
114 *FAT2* c.C10426T variant which creates a stop codon at p.R3476*. This variant was not found
115 in any of the controls, it is reported as a very rare variant in the gnomAD database and it is
116 likely deleterious according to the CADD prediction tool (Table 1). In addition, this patient was
117 also found to harbor a variant in *DCHS2*: c.836_837delAAinsG (p.K279Sfs*10), that creates a
118 frameshift resulting in premature termination of translation. This variant was not found in
119 any of the controls and was absent from the gnomAD database (Table 1).

120 Patient D140 was a 20.7-year-old female who was born full-term. She was diagnosed with
121 GHD following hypoglycemic seizures and received treatment with rGH (Table 2). Pituitary
122 MRI revealed EPP and possible PSIS (Figure 1B, Table 2). She was found to harbor a *DCHS2*
123 missense variant (p.T1328K) predicted to be damaging by all three prediction tools and has
124 not been reported previously (Table 1).

125 Patient D831 was a 15.1-year-old male who was born pre-term at 31 weeks of gestation due
126 to premature rupture of membranes. He was diagnosed with GH, TSH and partial ACTH
127 deficiency as well as learning difficulties. He received rGH therapy until the age of 15 years
128 and is now on replacement with Levothyroxine and steroids (Table 2). Pituitary MRI revealed
129 EPP and possible PSIS (Figure 1B, Table 2). Molecular analysis revealed a *FAT2* p.R1250H
130 missense variant absent from public databases, predicted as probably damaging by Polyphen,
131 damaging by SIFT and likely deleterious by CADD. This was reported as very rare in the
132 gnomAD database (Table 1).

133 Patient D205 was a 14.6-year-old male at the time of assessment. He was born at term with
134 cryptorchidism and micropenis. He was diagnosed with GH and TSH deficiency and placed
135 under replacement with rGH and Levothyroxine (Table 2). He also required testosterone
136 treatment for micropenis and for pubertal induction and maintenance. MRI revealed EPP
137 (Figure 1). He was found to harbor a *FAT2* missense variant (p.D2720H), not reported
138 previously, and predicted to be probably damaging by Polyphen, damaging by SIFT and likely
139 deleterious by CADD (Table 1).

140

141 **DCHS2 and FAT2 are expressed during embryonic pituitary development**

142 To explore whether the two genes contribute to pituitary development, we next examined
143 expression of *FAT2* and *DCHS2* proteins in the developing human pituitary by
144 immunostaining. At 17 post-conception weeks (pcw), *DCHS2* expression was detected in
145 mesenchymal cells around epithelial structures of the marginal zone as well as in diffuse
146 mesenchymal cells within the anterior lobe (arrows, Figure 2A). *FAT2* expression was also
147 detected in mesenchymal cells, but also in the posterior lobe and at low levels in epithelial
148 structures within the marginal zone (Figure 2B).

149 Specific cross-reactivity of the *FAT2* antibody allowed us to carry out analysis in the mouse
150 pituitary. At 14.5dpc, *FAT2* was abundantly detected in the mesenchyme surrounding the
151 developing gland, in invading mesenchymal tissue that will form the vasculature (4, 28), as
152 well as in cells at the external layer of the rostral RP (arrows) contacting the mesenchyme,
153 and in the infundibulum (arrowheads) (Figure 2C). Expression of *Fat2* and *Dchs2* in the
154 mesenchyme surrounding the developing RP and infundibulum was confirmed by mRNA in
155 situ hybridization (Supplementary Figure 1). At 18.5dpc just prior to birth, *FAT2* expression

156 remained strong in mesenchyme surrounding the pituitary; there was expression in the
157 posterior lobe and abundant signal detected throughout the vasculature of the anterior
158 lobe (Figure 2D). By 10-weeks in the adult mouse pituitary, FAT2 expression persisted in the
159 vasculature as confirmed by double immunofluorescence staining with Endomucin, marking
160 endothelial cells of the blood vessels (arrows, Figure 2E).

161

162 ***Dchs2*^{-/-} mouse mutants have defects in hypothalamic-pituitary development**

163 Considering the functional link suggested by the identification of PSIS patients with
164 putatively pathogenic *DCHS2* variants, we next sought to confirm such implication using a
165 *Dchs2* mutant mouse model. In order to confirm if *DCHS2* has a function during
166 hypothalamic-pituitary development, we analyzed *Dchs2*^{-/-} null mutants. Gross inspection of
167 the dissected mutant pituitary of neonates at P2 did not reveal any apparent morphological
168 anomalies compared to controls (Supplementary Figure 2A, n=9). At 18.5dpc, a stage when
169 morphogenesis of the HP axis has been fully achieved, and when PSIS-like anatomical
170 phenotypes can be unambiguously detected, embryos exhibited mild anterior pituitary
171 hypoplasia (3/6), accompanied by a significant reduction in the number of cycling cells as
172 determined by antibody staining against Ki-67 (average 26.3% cycling cells in controls
173 compared to 22.7% in mutants, $P=0.0044$ n=3, unpaired Student's t-test; Figure 3A).
174 Analysis of cycling cells in the marginal zone surrounding the cleft and separately in the
175 parenchyme revealed a reduction in both regions of mutants compared to controls
176 (marginal zone $P=0.0495$, parenchyme $P=0.007$). We next sought to determine if anterior
177 cell type commitment and differentiation occurred normally. Immunofluorescence staining
178 using antibodies against commitment markers PIT1 (POU1F1), SF1 (NR5A1), TPIT (TBX19) in

179 *Dchs2*^{-/-} and control *Dchs2*^{+/+} pituitaries did not reveal differences between genotypes
180 (Figure 3B), confirmed by qRT-PCR (Supplementary Figure 2B, n=4). Similarly, no differences
181 were observed for the expression of differentiation markers ACTH, GH and TSH (n=3, Figure
182 3B) or for the expression of the stem cell marker *Sox2* (Supplementary Figure 2B). These
183 results are consistent with a role for DCHS2 in controlling morphogenesis rather than cell
184 fate specification within the AP.

185 Histological examination of frontal sections at 18.5dpc at anterior axial levels,
186 revealed dysmorphology of the median eminence and developing pituitary stalk in a
187 proportion of the mutants (4/6). Of note, the pituitary stalk in mouse is very short compared
188 to the developing human pituitary. Mutant embryos exhibited invaginations in the median
189 eminence and the epithelium of the infundibular recess (arrowheads Figure 3C, two mutant
190 embryos shown, axial levels as indicated in the cartoon). None of these anomalies were
191 observed in control littermates (n=8).

192

193 ***Fat4*^{-/-} and *Dchs1*^{-/-} mutants exhibit additional morphogenetic defects of the anterior**
194 **pituitary**

195 The observation of variability in penetrance of the *Dchs2*^{-/-} null phenotypes suggested that
196 there might be some functional redundancy compensating for the loss of *Dchs2*. Indeed,
197 DCHS1 and DCHS2 act cooperatively during kidney development, acting with FAT4 as ligand-
198 receptor pair (24, 26). This led us to explore the possibility that other members of the
199 FAT/DCHS family might additionally contribute to pituitary development. We previously
200 detected strong expression of *Fat4* in the rostral tip of the developing murine pituitary
201 (which develops into the pars tuberalis), and strong expression of *Dchs1* in surrounding

202 mesenchyme (27). To characterize their expression during late pituitary development we
203 carried out RNAscope mRNA *in situ* hybridization using specific probes against *Fat4* and
204 *Dchs1* in sagittal sections through wild type pituitaries at 18.5dpc. *Fat4* expression was
205 strong in the developing pars tuberalis, the developing posterior lobe and pituitary stalk,
206 and transcripts were also detected in the surrounding mesenchyme and scattered cells of
207 the developing anterior lobe. Low levels of *Dchs1* transcripts were detected throughout
208 these tissues with the highest expression in the pituitary stalk (Figure 4A). To investigate if
209 *Dchs1* expression increases in *Dchs2*^{-/-} mutants, indicative of a compensatory mechanism,
210 we carried out qRT-PCR on whole pituitary lysates comparing *Dchs2*^{-/-} and *Dchs2*^{+/-} control
211 genotypes. Although not significant with the available samples, there appears to be an
212 elevation of *Dchs1* mRNA levels in *Dchs2*^{-/-} mutants (Supplementary Figure 2B, n=4 per
213 genotype).

214 We hypothesized that loss of FAT4 or DCHS1 could also lead to pituitary defects. As
215 neither *Fat4*^{-/-} or *Dchs1*^{-/-} mutants are viable past the early postnatal period, analysis was
216 limited to embryonic stages and the perinatal period (P0-P2). As in *Dchs2*^{-/-} mutants,
217 histological analysis of *Fat4*^{-/-} mutants at 13.0dpc revealed abnormal invaginations in the
218 epithelium of the infundibular recess in 7/10 embryos (arrowheads in Figure 4B). We also
219 observed a severely abnormal invagination of the infundibulum lacking a central lumen,
220 using mRNA *in situ* hybridization against *Fat3* to mark infundibular tissue (27) (1/10
221 embryos, Figure 4C). These infundibular anomalies were not observed in *Dchs1*^{-/-} embryos
222 (0/5 at 13.0dpc). The infundibular phenotypes shared between *Fat4*^{-/-} and *Dchs2*^{-/-} mutants
223 suggest that FAT4 may be acting in concert with DCHS2, as receptor-ligand pair, during
224 posterior pituitary development.

225 Upon gross examination at P0, both *Fat4*^{-/-} and *Dchs1*^{-/-} pituitaries exhibited
226 shortening of the medio-lateral axis of the anterior pituitary compared to wild type
227 littermates (Figure 4C), unlike *Dchs2*^{-/-} mutants which did not display this phenotype (n=9,
228 Supplementary Figure 2A). The size of the intermediate and posterior lobes was comparable
229 to wild type controls (n=8 for *Fat4*^{-/-}, n=10 for *Dchs1*^{-/-}). Analysis of proliferation by Ki-67
230 immunostaining did not reveal differences in the number of cycling cells between genotypes
231 (Supplementary Figure 3, n=3 per genotype). Immunofluorescence staining of lineage
232 commitment and differentiation markers of the anterior pituitary (PIT1, SF1, TPIT, GH, TSH,
233 ACTH) identified normal distribution of committed and differentiated cell types in *Fat4*^{-/-}
234 pituitaries compared to controls (n=3, Figure 4D). No differences were observed between
235 *Fat4*^{-/-} and *Dchs1*^{-/-} genotypes (not shown).

236

237 **Discussion**

238 Screening 28 patients with EPP and/or PSIS, we have identified seven variants in *FAT2* and
239 *DCHS2* in six patients. Five of these variants were predicted to be damaging by *in silico*
240 analysis. Indeed, the existence of familial cases with mutations and/or single nucleotide
241 variants in genes involved in the developmental process such as in *HESX1*, *LHX4*, *PROP1*,
242 *OTX2*, *SOX3*, *PROKR2* and *GPR161* have suggested a Mendelian form of inheritance (6, 7,
243 29). Recently, Zwaveling-Soonawala et al, also identified *DCHS1* as one of the candidate
244 genes for sporadic PSIS in two young patients: a nine year old female who presented with
245 absent stalk and anterior pituitary, EPP and hormonal deficiencies and a 2.5 year old male
246 with small stalk and anterior pituitary, EPP and hormonal deficiencies (8). Although no
247 functional studies were performed, both these patients had variants in other genes that

248 were also predicted to be damaging, such as in *GLI2* which has been reported to be involved
249 in holoprosencephaly and abnormal pituitary development (30) and in *BMP4*, which has a
250 crucial role during embryonic pituitary development (31) indicating that variants in one or
251 more genes other than *FAT2* and *DCHS2* may be required for an apparent phenotype.

252 In our screen, all patients with *FAT2* or *DCHS2* variants had GHD and three of them had
253 combined hormone deficiency. Two of these patients had a more severe phenotype with
254 complete deficiency of the adenohypophysis and a pituitary height smaller than expected
255 for their age and sex.

256 Considering that in all *Dchs* and *Fat* mouse mutants analyzed, anterior cell type
257 commitment and differentiation occurred normally, the hormonal deficiencies identified in
258 our patients could be due to the lack of trophic signals of the hypothalamic releasing factors
259 rather than defects in the differentiation of the anterior endocrine cells. In the patients, we
260 were not able to identify a specific phenotype-genotype correlation, which indicates that
261 these variants can be confounding factors, or causative where other factors also contribute
262 to the severity of symptoms.

263 Expression analysis of both mouse and human tissue revealed that in development,
264 *FAT/DCHS* protocadherins are expressed in the mesenchyme surrounding the pituitary. The
265 infundibulum and posterior pituitary gland receive a rich blood supply from the superior
266 hypophyseal artery, infundibular artery and inferior hypophyseal artery (32), all of
267 mesenchymal origin (28, 33). Disruption of the pituitary vascular network can result in
268 abnormal tissue morphology and poor function (28, 33). We postulate that mutations in
269 *FAT2* and *DCHS2* may affect the development of the posterior lobe and its connection to the
270 hypothalamus, through affecting the surrounding mesenchymal contribution. By analyzing

271 developing *Dchs2*^{-/-} mouse mutant pituitaries, we have identified a partially penetrant
272 pituitary stalk defect as well as anterior pituitary hypoplasia. Like *Fat2*^{-/-} mice however,
273 these have previously been described as normal, healthy and viable, possibly due to the
274 redundant roles with other FAT and DCHS family members (26, 34). Consistent with this
275 stalk phenotype, we also identified abnormal infundibular development in *Fat4*^{-/-} mutants,
276 previously shown to exhibit poor cerebral neuronal migration (14, 35). As such, the ventral
277 migration of axons of hypothalamic neurons located in the paired supraoptic and
278 paraventricular nuclei, which terminate in the posterior pituitary (4), might also be affected
279 by loss of FAT/DCHS protocadherins, resulting in abnormal evagination of this tissue and
280 PSIS.

281 Interestingly, analysis of *Fat4*^{-/-} as well as *Dchs1*^{-/-} single mutants revealed an
282 additional pituitary defect, shortening of the medio-lateral axis of the anterior lobe. As this
283 is consistent between the two genotypes, we conclude that FAT4 and DCHS1, expressed in
284 the developing RP, infundibulum and surrounding mesenchyme (27), are likely acting as
285 receptor-ligand pair in the morphogenesis of the anterior lobe, and we hypothesize that
286 expression of both proteins in the surrounding mesenchyme is critical for this process (27).
287 FAT4/DCHS1 may be involved in cell movements during development, which is consistent
288 with their known role in planar cell polarity (10, 11, 25), often an important pathway during
289 dynamic rearrangement and migration of cells. In the anterior pituitary they are unlikely to
290 act upstream of YAP for this purpose, as previous work deregulating YAP levels during
291 development did not result in medio-lateral morphogenesis defects (36).

292 Taken together, our studies have revealed a requirement for the concerted action of
293 FAT/DCHS protocadherins for normal pituitary development and support the pathogenicity

294 of *FAT2* and *DCHS2* variants in patients with ectopic PSIS in addition to other genes reported
295 (8). As PSIS may present with isolated or multiple hormonal deficiencies, then neonatal
296 hypoglycemia, micropenis and/or cryptorchidism with or without growth deficit should
297 prompt early screening with hormonal and imaging investigations for early detection and
298 treatment. Furthermore, genetic screening for identification of a specific mutation in the
299 genes involved in PSIS development is a prerequisite for genetic counseling and appropriate
300 long-term follow-up, which is imperative as there is a strong possibility of development of
301 other hormonal insufficiencies.

302 **Methods**

303 **Whole exome sequencing of patients with ectopic posterior pituitary**

304 The data from 28 unrelated patients diagnosed with non-syndromic EPP were reviewed and
305 DNA was extracted from peripheral blood mononuclear cells. Whole exome sequencing and
306 variant calling were performed for *FAT1*, *FAT2*, *FAT3*, *FAT4*, *DCHS1* and *DCHS2*. DNA samples
307 from 156 in-house parents of osteosarcoma patients and 8,554 from Atherosclerosis Risk in
308 Communities Study (ARIC) database were used as controls.

309 **Analysis of the identified variants**

310 The variants that were identified in controls were filtered and analysis was focused on the
311 variants with functional type “high” and “moderate”. Allele frequencies identified in
312 patients with EPP were compared to allele frequency published on reference database The
313 Genome Aggregation Database (gnomAD) spans 125,748 exome sequences and 15,708
314 whole-genome sequences from unrelated individuals and publicly available online
315 (<https://gnomad.broadinstitute.org>). The possible functional impact of an amino acid
316 substitution was predicted by three different in silico prediction tools: (1) the PolyPhen
317 (Polymorphism Phenotyping) program (<http://genetics.bwh.harvard.edu/pph2>) which
318 calculates the position-specific independent counts (PSIC) score that represents the
319 probability that a substitution be damaging; values nearer to 1 are more confidently
320 predicted to be deleterious, (2) for missense variants, the Sorting Intolerant From Tolerant
321 (SIFT) program [<http://sift.jcvi.org>] calculates normalized probabilities for all possible
322 substitutions from the alignment. Positions with normalized probabilities less than 0.05 are
323 predicted to be deleterious; those greater than or equal to 0.05 are predicted tolerated. (3)

324 The Combined Annotation Dependent Depletion score (CADD, v1.3,
325 <https://www.ncbi.nlm.nih.gov/pubmed/30371827>) which combines deleteriousness
326 predictions from multiple algorithms into a single phred-like score for all possible single
327 nucleotide variants in the genome (i.e. a CADD score >10 is predicted to be amongst the top
328 10% most deleterious single nucleotide variants in the genome, CADD score >20 is amongst
329 the top 1%, CADD score >30 is amongst the top 0.1%, etc). For convenience we classified the
330 variants with a CADD score >20 as 'likely deleterious' and below 20 as 'likely benign'.

331 **Animals**

332 *Dchs2*^{-/-}, *Fat4*^{fl/fl} and *Dchs1*^{-/-} animals were previously described (24-26). For the generation
333 of *Fat4*^{-/-} animals, *Fat4*^{fl/fl} mice were crossed with the *Actb*^{Cre/+} strain for ubiquitous deletion
334 (37) and offspring were intercrossed. For embryo collection, the morning of vaginal plug was
335 considered 0.5dpc. Embryos or postnatal pituitaries were dissected, fixed in 10% NBF
336 overnight with agitation, then dehydrated through an ascending ethanol series. Tissues
337 were processed for paraffin embedding and sectioned to 4µm for RNAscope mRNA *in situ*
338 hybridization, or 7µm for hematoxylin and eosin staining and immunofluorescence.

339 **Hematoxylin and eosin staining**

340 Slides were dewaxed in HistoClear (National Diagnostics) and rehydrated through a
341 descending ethanol series in dH₂O. Sections were stained with Harris' hematoxylin and
342 eosin following standard protocols. Slides were dehydrated and dried, then coverslips
343 mounted with VectaMount (Vector Ltd).

344 **RNAscope mRNA *in situ* hybridization**

345 Sections were processed and stained as described previously (27). Briefly, slides were
346 heated to 60°C, dewaxed in xylene and washed in 100% ethanol and processed following
347 the RNAscope 2.5HD Reagent Kit-RED assay kit (Advanced Cell Diagnostics) with specific
348 probes (*Fat4*, *Dchs1*, *Fat3*). Following detection, slides were weakly counterstained with
349 hematoxylin and coverslips mounted with VectaMount (Vector Ltd).

350 **Immunofluorescence (IMF)**

351 Slides were deparaffinized in HistoClear, rehydrated through a descending ethanol series,
352 followed by antigen retrieval in pH6.0 citrate buffer in a NXGEN Decloaking Chamber
353 (Menari Diagnostics) at 110°C for 3min. Slides were washed in PBST (PBS with 0.1% Triton-
354 X), blocked in Blocking Buffer (0.15% glycine, 2mg/ml BSA, 0.1% Triton-X in PBS) with 10%
355 sheep serum for 1h at room temperature, then incubated overnight in primary antibody in
356 Blocking Buffer with 1% sheep serum at 4°C. Primary antibodies used were against: DCHS2
357 (1:500, Atlas HPA064159), FAT2 (1:1000, Santa Cruz sc59985), Ki-67 (1:300, Abcam
358 ab16667), SOX2 (1:300, Abcam ab97959), PIT1 (1:1000, gift from Prof. S. Rhodes, University
359 of North Florida, USA), TPIT (1:300, gift from Prof. J. Drouin, University of Montreal,
360 Canada), SF1 (1:300, Life Technologies N1665), ACTH (1:300, Fitzgerald 10C-CR1096M1), GH
361 (1:1000, NHPP AFP5641801), TSH (1:1000 NHPP AFP-1274789). The Vector ImmPRESS kit
362 was used for antibodies against SF1 according to the manufacturer's instructions. The
363 PerkinElmer TSA kit was used for antibodies against DCHS2 and FAT2, as previously
364 described (36). After primary antibody incubation, slides were washed in PBST then
365 incubated with appropriate secondary antibodies (biotinylated goat anti-rabbit (1:300,
366 Abcam ab6720), biotinylated goat anti-mouse (1:300 Abcam ab6788)), and incubated with
367 fluorophore-conjugated Streptavidin (1:500, Life Technologies S11223) for 1h at room

368 temperature. Quenching of endogenous autofluorescence was carried out by treatment
369 with Sudan Black B following immunofluorescence against TPIT and SF1. Nuclei were
370 counterstained with Hoechst (1:10000, Life Technologies H3570). Coverslips were mounted
371 with VectaMount (Vector Laboratories, H1000).

372 **Imaging**

373 Wholemount images were taken with a MZ10 F Stereomicroscope (Leica Microsystems),
374 using a DFC3000 G camera (Leica Microsystems). For bright field images, stained slides were
375 scanned with Nanozoomer-XR Digital slide scanner (Hamamatsu) and images processed
376 using Nanozoomer Digital Pathology View. Immunofluorescent staining was imaged with a
377 TCS SP5 confocal microscope (Leica Microsystems) and images processed using Fiji (38).

378 **Proliferation analysis**

379 The number of Ki-67 positive cells and total nuclei stained with Hoechst, were counted
380 manually using Fiji (at least 5000 nuclei counted over 5-7 sections per biological sample) for
381 control and mutant pituitaries, n=3 per genotype. Nuclei along the marginal zone epithelium
382 were recorded separately to those within the anterior pituitary parenchyme.

383 **Quantitative RT-PCR**

384 Whole pituitaries were dissected from 10 week old *Dchs2^{+/-}* (control) and *Dchs2^{-/-}* (mutant)
385 mice and placed in RNAlater-ice (Thermo Fisher, AM7030). They were flash frozen in liquid
386 nitrogen and stored at -80°C. mRNA was extracted using Monarch Total RNA Miniprep kit
387 (New England Biolabs, T2010S), translated using QuantiTect Reverse Transcription kit
388 (Qiagen, 205311) then qRT-PCR was performed using QuantiNova SYBR Green RT-PCR kit
389 (Qiagen, 208152) on a Roche Lightcycler 480. Data were analyzed using delta delta CT

390 method normalized to housekeeping gene expression, n=4 pituitaries per genotype. Primers
391 used: *Pou1f1* (*Pit1*) fw CACGGCTCAGAATTCAGTCA, rv TCCAGAGCATCCTTAGCAGC; *Tbx19*
392 (*Tpit*) fw TGTCTCGCCTGCTTAACGTG, rv GACAGGGAACATCCGTCTGC; *Nr5a1* (*Sf1*) fw
393 AGCTGCAAGGGCTTCTTCAA, rv CATTTCGATCAGCAGCACAG; *Sox2* fw
394 GAGGGCTGGACTGCGAACT, rv TTTGCACCCCTCCCAATTC; *Dchs1* fw
395 TCCACGTTTCATCCACTCAGC, rv GGGGACTGTTCTCACGAAGG; *Hprt* (housekeeping) fw
396 GTTGGGCTTACCTCACTGCT, rv TCATCGCTAATCACGACGCT; *Actb* (housekeeping) fw
397 TTCTTTGCAGCTCCTTCGTT, rv ATGGAGGGGAATACAGCCC.

398 **Statistics**

399 Data were analyzed using two-tailed unpaired Student's t-tests using the Holm-Sidak
400 method to correct for multiple analysis, where $P < 0.05$ was taken to be statistically
401 significant.

402 **Study Approval**

403 All participants, or their legal guardian, provided written and informed consent. The present
404 studies in humans were reviewed and approved by the Irmandade da Santa Casa de
405 Misericórdia de São Paulo review board (project number 34003914.0.0000.5479), located at
406 Marquês de Itu Street, 381, São Paulo, Brazil. Animal husbandry was carried out under
407 compliance of the Animals (Scientific Procedures) Act 1986, relevant Home Office License
408 (P5F0A1579) and KCL Ethical Review approval.

409

410 **AUTHOR CONTRIBUTIONS**

411 Designing research studies: FH, CAS, CLA; conducting experiments: EJL, PX, AS, TSS, FRF, DS,
412 ALP; acquiring data: EJL, PX, TSS, CK, CAL, AS, JLM, NP, JL, CLA; analyzing data: EJL, PX, AS, FRF;
413 providing reagents: TH, PF-W, FH, CAS; writing the manuscript: PX, EJL, CLA; editing the
414 manuscript: PF-W, FH, JLM, CAS.

415

416 **ACKNOWLEDGEMENTS**

417 We thank the patients and their families for participating in the described studies. This study
418 was supported by grants MR/L016729/1 from the MRC (CLA), a Lister Institute Research
419 Prize Fellowship to CLA, RG130699 from The Royal Society (CLA), the Deutsche
420 Forschungsgemeinschaft (DFG) within the 314061271 - TRR 205 (CLA), the AFM-Téléthon
421 (Association Française contre les myopathies) grant 20861 (FH), grant BB/M022544/1 from
422 the BBSRC (PF-W). This study was in part funded by the intramural research program of the
423 *Eunice Kennedy Shriver* National Institute of Child Health of Human Development (NICHD),
424 Bethesda, MD20892, USA. We are grateful to Prof. Jacques Drouin and Prof. Simon Rhodes
425 for TPIT and PIT antibodies respectively, and the National Hormone and Peptide Program
426 (Harbor-University of California, Los Angeles Medical Center) for providing some of the
427 hormone antibodies used in this study. We thank Prof. Kenneth Irvine for continued advice
428 and sharing reagents and Prof. Helen McNeill for providing the *Fat4* mouse mutant.

429

430 **References**

- 431 1. Bar C, et al. Pituitary Stalk Interruption Syndrome from Infancy to Adulthood: Clinical,
432 Hormonal, and Radiological Assessment According to the Initial Presentation. *PloS one*.
433 2015;10(11):e0142354.

- 434 2. Voutetakis A, Sertedaki A, Dacou-Voutetakis C. Pituitary stalk interruption syndrome:
435 cause, clinical manifestations, diagnosis, and management. *Current opinion in*
436 *pediatrics*. 2016;28(4):545-550.
- 437 3. Fujisawa I, et al. Transection of the pituitary stalk: development of an ectopic posterior
438 lobe assessed with MR imaging. *Radiology*. 1987;165(2):487-489.
- 439 4. Cheung LY, Davis SW, Brinkmeier ML, Camper SA, Perez-Millan MI. Regulation of
440 pituitary stem cells by epithelial to mesenchymal transition events and signaling
441 pathways. *Mol Cell Endocrinol*. 2017;445:14-26.
- 442 5. Tatsi C, et al. Pituitary stalk interruption syndrome and isolated pituitary hypoplasia may
443 be caused by mutations in holoprosencephaly-related genes. *J Clin Endocrinol Metab*.
444 2013;98(4):E779-784.
- 445 6. Reynaud R, et al. PROKR2 variants in multiple hypopituitarism with pituitary stalk
446 interruption. *J Clin Endocrinol Metab*. 2012;97(6):E1068-1073.
- 447 7. Reynaud R, et al. Pituitary stalk interruption syndrome in 83 patients: novel HESX1
448 mutation and severe hormonal prognosis in malformative forms. *European journal of*
449 *endocrinology*. 2011;164(4):457-465.
- 450 8. Zwaveling-Soonawala N, et al. Clues for Polygenic Inheritance of Pituitary Stalk
451 Interruption Syndrome From Exome Sequencing in 20 Patients. *J Clin Endocrinol Metab*.
452 2018;103(2):415-428.
- 453 9. Tanoue T, Takeichi M. New insights into Fat cadherins. *Journal of cell science*.
454 2005;118(Pt 11):2347-2353.
- 455 10. Mao Y, et al. Dchs1-Fat4 regulation of polarized cell behaviours during skeletal
456 morphogenesis. *Nature communications*. 2016;7:11469.
- 457 11. Zakaria S, et al. Regulation of neuronal migration by Dchs1-Fat4 planar cell polarity.
458 *Current biology : CB*. 2014;24(14):1620-1627.
- 459 12. Ragni CV, et al. Amotl1 mediates sequestration of the Hippo effector Yap1 downstream
460 of Fat4 to restrict heart growth. *Nature communications*. 2017;8:14582.
- 461 13. Crespo-Enriquez I, et al. Dchs1-Fat4 regulation of osteogenic differentiation in mouse.
462 *Development (Cambridge, England)*. 2019;146(14).
- 463 14. Cappello S, et al. Mutations in genes encoding the cadherin receptor-ligand pair DCHS1
464 and FAT4 disrupt cerebral cortical development. *Nature genetics*. 2013;45(11):1300-
465 1308.
- 466 15. Blair S, McNeill H. Big roles for Fat cadherins. *Current opinion in cell biology*. 2018;51:73-
467 80.
- 468 16. Rock R, Schrauth S, Gessler M. Expression of mouse dchs1, fjx1, and fat-j suggests
469 conservation of the planar cell polarity pathway identified in *Drosophila*. *Developmental*

- 470 *dynamics : an official publication of the American Association of Anatomists.*
471 2005;234(3):747-755.
- 472 17. Ivanovski I, et al. Van Maldergem syndrome and Hennekam syndrome: Further
473 delineation of allelic phenotypes. *American journal of medical genetics Part A.*
474 2018;176(5):1166-1174.
- 475 18. Alders M, et al. Hennekam syndrome can be caused by FAT4 mutations and be allelic to
476 Van Maldergem syndrome. *Human genetics.* 2014.
- 477 19. Mansour S, et al. Van Maldergem syndrome: further characterisation and evidence for
478 neuronal migration abnormalities and autosomal recessive inheritance. *European*
479 *journal of human genetics : EJHG.* 2012;20(10):1024-1031.
- 480 20. Zampino G, et al. Cerebro-facio-articular syndrome of Van Maldergem: confirmation of
481 a new MR/MCA syndrome. *Clinical genetics.* 1994;45(3):140-144.
- 482 21. van Maldergem L, Wetzburger C, Verloes A, Fourneau C, Gillerot Y. Mental retardation
483 with blepharo-naso-facial abnormalities and hand malformations: a new syndrome?
484 *Clinical genetics.* 1992;41(1):22-24.
- 485 22. Hennekam RC, et al. Autosomal recessive intestinal lymphangiectasia and lymphedema,
486 with facial anomalies and mental retardation. *American journal of medical genetics.*
487 1989;34(4):593-600.
- 488 23. Sotos J, et al. A patient with van Maldergem syndrome with endocrine abnormalities,
489 hypogonadotropic hypogonadism, and breast aplasia/hypoplasia. *International journal*
490 *of pediatric endocrinology.* 2017;2017:12.
- 491 24. Mao Y, et al. Characterization of a Dchs1 mutant mouse reveals requirements for Dchs1-
492 Fat4 signaling during mammalian development. *Development (Cambridge, England).*
493 2011;138(5):947-957.
- 494 25. Saburi S, et al. Loss of Fat4 disrupts PCP signaling and oriented cell division and leads to
495 cystic kidney disease. *Nature genetics.* 2008;40(8):1010-1015.
- 496 26. Bagherie-Lachidan M, et al. Stromal Fat4 acts non-autonomously with Dachshous1/2 to
497 restrict the nephron progenitor pool. *Development (Cambridge, England).* 2015.
- 498 27. Lodge EJ, Russell JP, Patist AL, Francis-West P, Andoniadou CL. Expression Analysis of
499 the Hippo Cascade Indicates a Role in Pituitary Stem Cell Development. *Frontiers in*
500 *physiology.* 2016;7:114.
- 501 28. Davis SW, et al. beta-catenin is required in the neural crest and mesencephalon for
502 pituitary gland organogenesis. *BMC developmental biology.* 2016;16(1):16.
- 503 29. Fang Q, et al. Genetics of Combined Pituitary Hormone Deficiency: Roadmap into the
504 Genome Era. *Endocrine reviews.* 2016;37(6):636-675.

- 505 30. Arnhold IJ, Franca MM, Carvalho LR, Mendonca BB, Jorge AA. Role of GLI2 in
506 hypopituitarism phenotype. *J Mol Endocrinol*. 2015;54(3):R141-150.
- 507 31. Ericson J, Norlin S, Jessell TM, Edlund T. Integrated FGF and BMP signaling controls the
508 progression of progenitor cell differentiation and the emergence of pattern in the
509 embryonic anterior pituitary. *Development (Cambridge, England)*. 1998;125(6):1005-
510 1015.
- 511 32. Ciofi P, et al. Brain-endocrine interactions: a microvascular route in the mediobasal
512 hypothalamus. *Endocrinology*. 2009;150(12):5509-5519.
- 513 33. Scully KM, et al. Epithelial cell integrin β 1 is required for developmental angiogenesis in
514 the pituitary gland. *Proceedings of the National Academy of Sciences*.
515 2016;113(47):13408-13413.
- 516 34. Barlow JL, et al. A p53-dependent mechanism underlies macrocytic anemia in a mouse
517 model of human 5q- syndrome. *Nature medicine*. 2010;16(1):59-66.
- 518 35. Zakaria S, et al. Regulation of neuronal migration by dchs1-fat4 planar cell polarity.
519 *Current biology : CB*. 2014;24(14):1620-1627.
- 520 36. Lodge EJ, et al. Homeostatic and tumourigenic activity of SOX2+ pituitary stem cells is
521 controlled by the LATS/YAP/TAZ cascade. *eLife*. 2019;8.
- 522 37. Lewandoski M, Meyers EN, Martin GR. Analysis of Fgf8 gene function in vertebrate
523 development. *Cold Spring Harb Symp Quant Biol*. 1997;62:159-168.
- 524 38. Schindelin J, et al. Fiji: an open-source platform for biological-image analysis. *Nature*
525 *methods*. 2012;9(7):676-682.

526

527 **Figure 1. Variants in FAT2 and DCHS2 in patients with PSIS.** (A) Representative schematic of
528 the FAT2 and DCHS2 proteins indicating the locations of identified mutations. Variants in
529 red are predicted likely deleterious by CADD score (>20). No CADD score data available for
530 DCHS2 p.K279Sfs*10. (B) Sagittal T1 pituitary MRIs of the six patients with *FAT2/DCHS2*
531 variants and normal MRI for comparison, bottom left. For each patient, the normal posterior
532 pituitary bright spot is not seen in the pituitary fossa, rather, an ectopic small region of high
533 T1 signal at the top of the infundibulum or higher (red arrows). PS: pituitary stalk, AP:
534 anterior pituitary, PP: posterior pituitary (normal intrasellar).

535

536

537

538

539

540

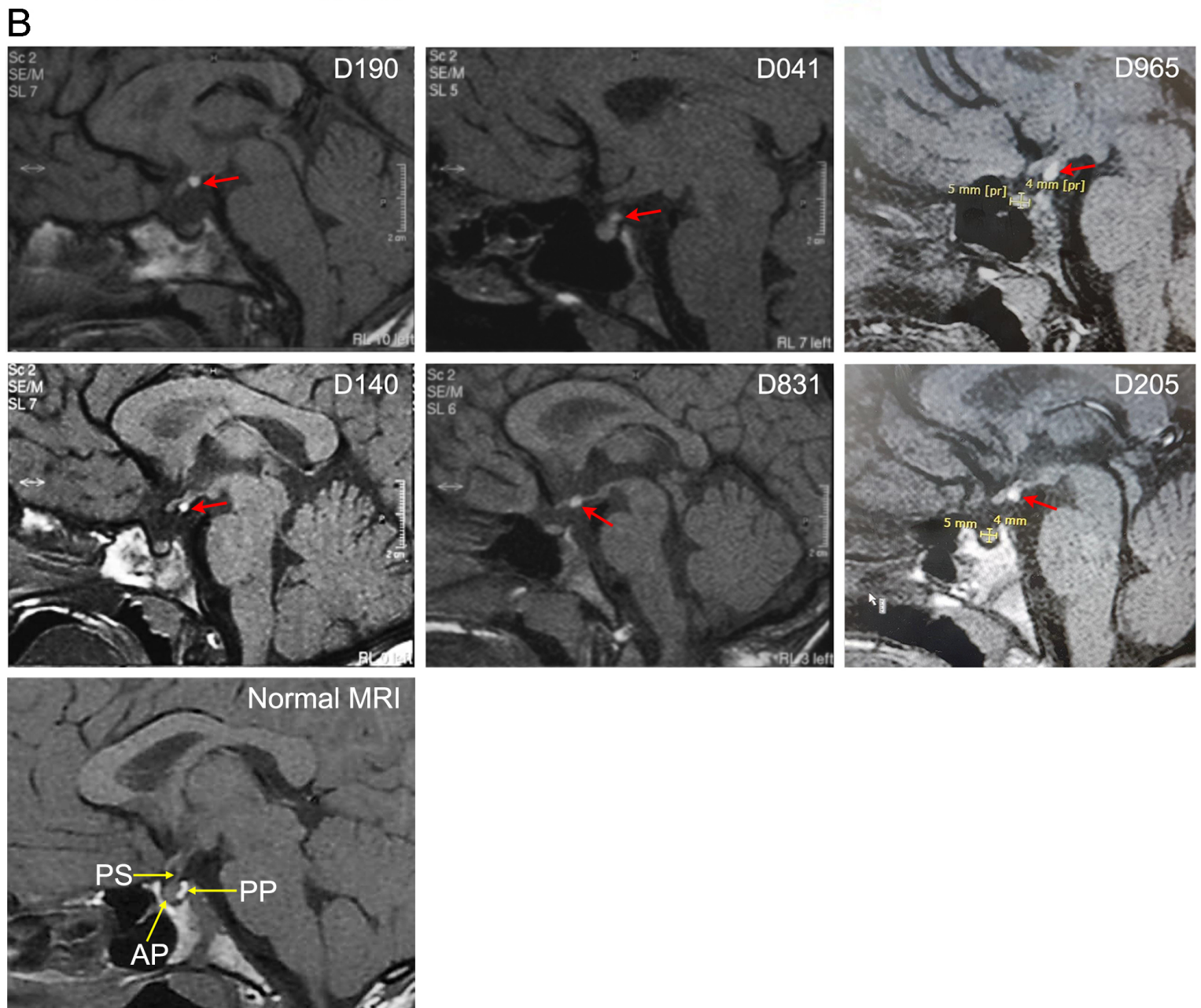
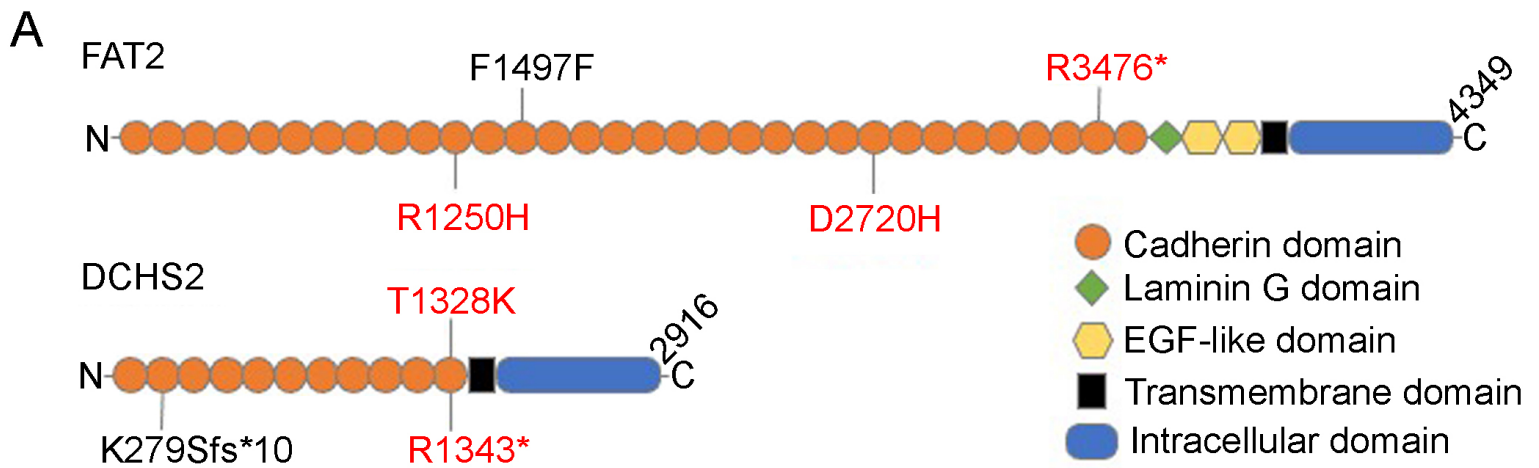
541

542

543

544

545



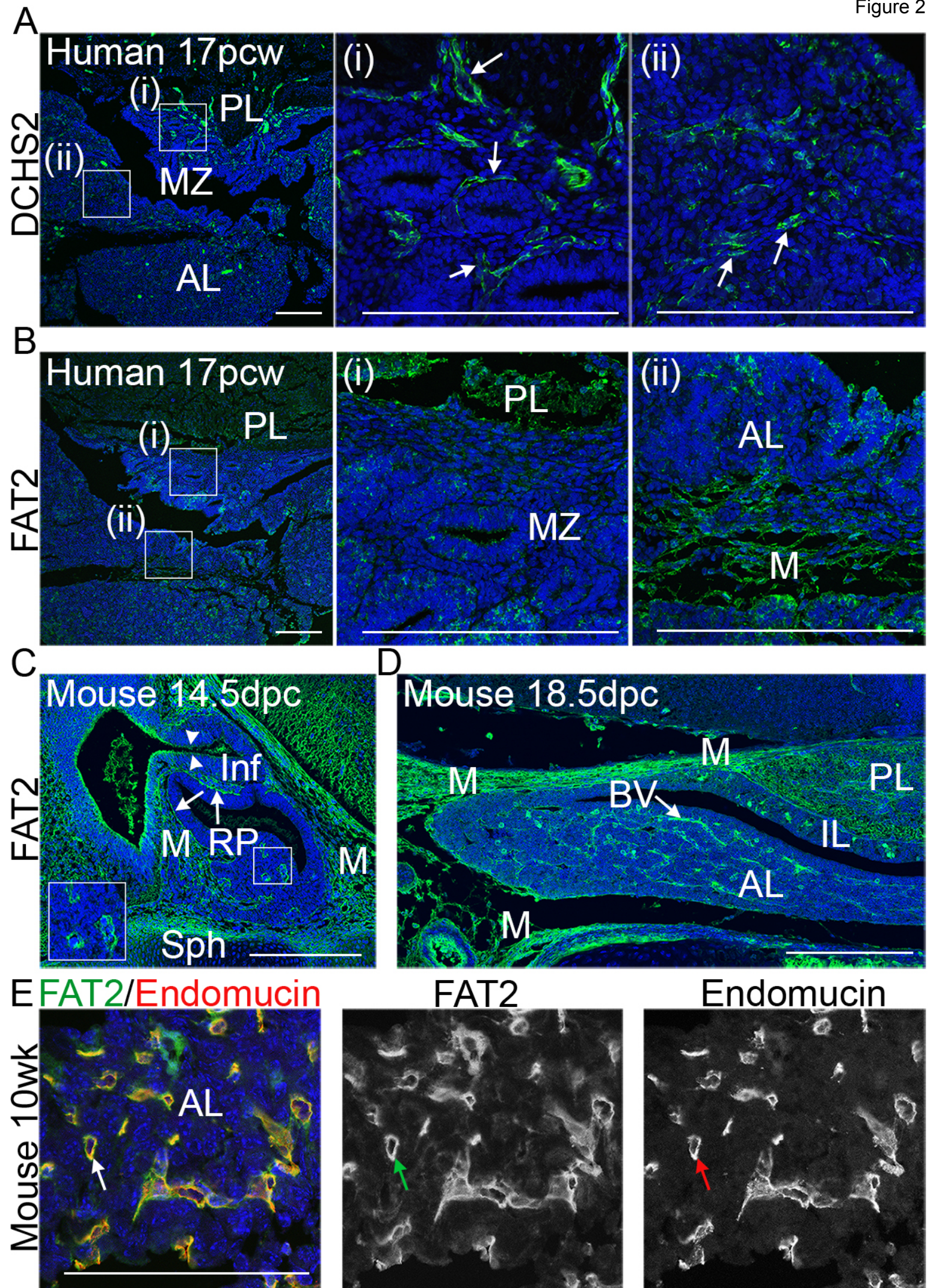
547 **Figure 2. DCHS2 and FAT2 expression in the developing pituitary. (A,B)**

548 Immunofluorescence staining on 17 post-conception week (pcw) human fetal pituitary
549 sections, using specific antibodies against DCHS2 (A) and FAT2 (B), n=2. DCHS2 is expressed
550 in mesenchymal tissues surrounding epithelial structures in the marginal zone, between the
551 posterior and anterior pituitary and within the anterior lobe (arrows). FAT2 localizes in
552 mesenchymal tissues within the anterior lobe, is expressed throughout the posterior lobe
553 and diffuse staining is observed in epithelial structures in the marginal zone. Images in (i)
554 and (ii) are magnified boxed regions in (A) and (B). **(C,D)** Immunofluorescence staining using
555 antibodies against FAT2 on the developing mouse pituitary at 14.5 days post coitum (dpc)
556 (C) and 18.5dpc (D), n=3. At 14.5dpc FAT2 localizes in mesenchymal tissue Rathke's pouch
557 (RP), in cells of (RP) making contact with the mesenchyme (arrows) and in cells of the
558 infundibulum (arrowheads) (C). At 18.5dpc, FAT2 expression persists in the mesenchyme
559 surrounding the gland, throughout the posterior lobe and in vasculature throughout the
560 anterior lobe (D). **(E)** In the wild type adult pituitary at 10 weeks, FAT2 (green) is expressed
561 strongly by cells of the vasculature, as seen by double-immunofluorescence staining with
562 Endomucin (red) marking endothelial cells (E), n=3. PL: posterior lobe, AL: anterior lobe, IL:
563 intermediate lobe, MZ: marginal zone, Inf: infundibulum, RP: Rathke's pouch, M:
564 mesenchyme, Sph: sphenoid bone, BV: blood vessels. Scale bars: 200µm in (A-C), 100µm in
565 (E).

566

567

568

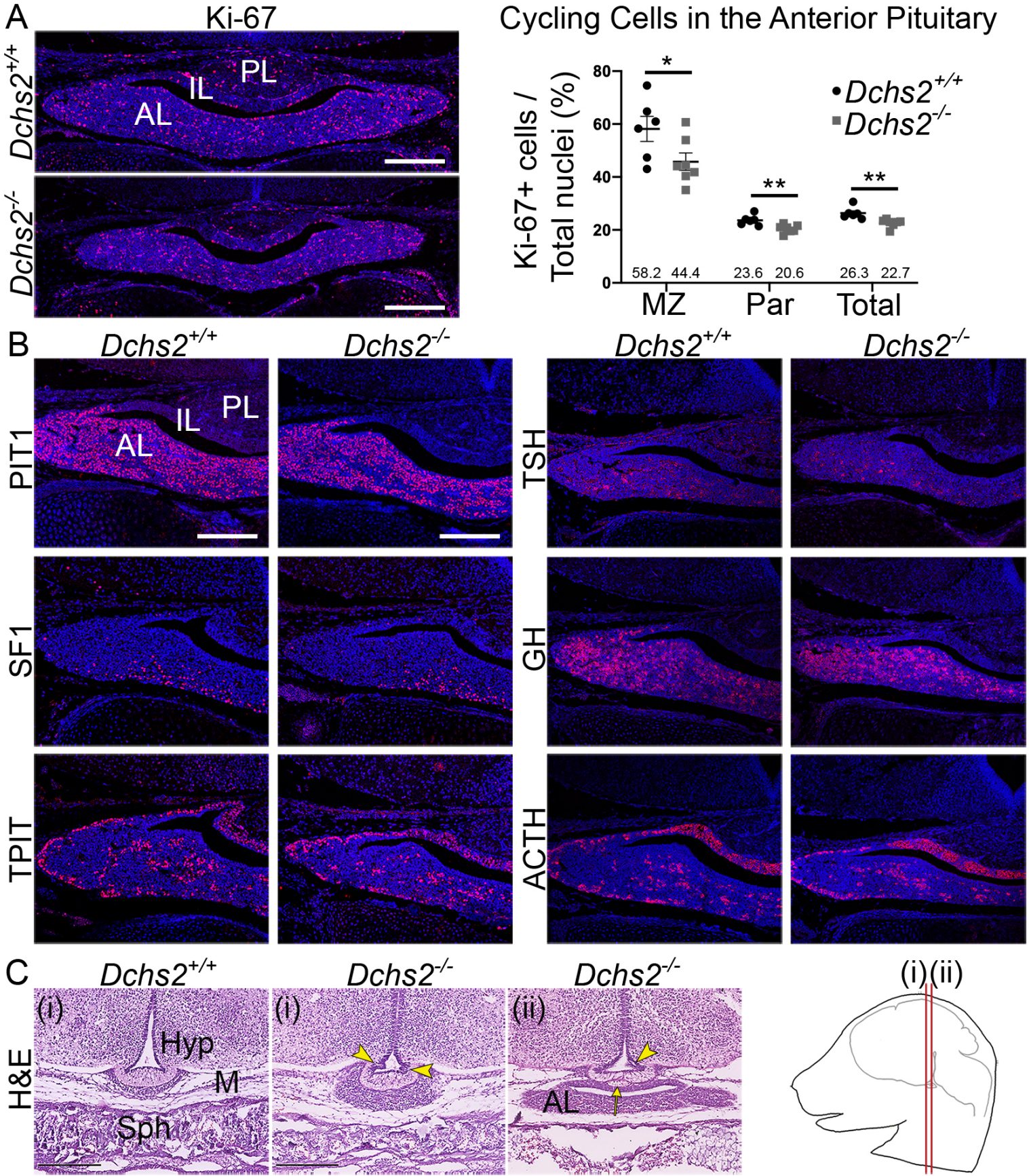


570 **Figure 3. DCHS2 is required for normal murine pituitary development. (A)**
571 Immunofluorescence staining using antibodies against Ki-67 to detect cycling cells, on
572 frontal sections of pituitaries from *Dchs2*^{-/-} mutants and wild type littermate controls at
573 18.5dpc. Graph depicting quantification of cycling cells of the anterior pituitary of wild type
574 controls and *Dchs2*^{-/-} mutants, showing reduced proliferation in mutants in the marginal
575 zone (MZ) surrounding the cleft $P=0.0495$, parenchyme (Par) $P=0.007$ and total throughout
576 the anterior lobe $P=0.0044$, unpaired Student's t-test (n=3 per genotype, multiple sections
577 counted). Values of Ki-67 positive cells are expressed as a percentage of the total nuclei in
578 the anterior lobe. Average values are indicated. **(B)** Immunofluorescence staining on *Dchs2*^{-/-}
579 pituitaries and littermate controls at 18.5dpc (n=3) using antibodies against lineage-
580 committed progenitor markers PIT1 (thyrotrophs, somatotrophs, lactotrophs), SF1
581 (gonadotrophs) and TPIT (corticotrophs, melanotrophs) and hormones TSH, GH and ACTH
582 expressed in differentiated thyrotrophs, somatotrophs and corticotrophs, respectively.
583 Staining is comparable for all markers between genotypes. **(C)** Hematoxylin and eosin
584 staining on frontal sections of *Dchs2*^{-/-} mutants and control at 18.5dpc at axial levels as
585 indicated in the cartoon (n=6). Abnormal invaginations are seen in the median eminence
586 (arrowheads) as wells as lobulated protrusions (arrow). PL: posterior lobe, IL: intermediate
587 lobe, AL: anterior lobe, Hyp: hypothalamus, M: mesenchyme, Sph: sphenoid bone. Scale
588 bars: 200 μ m in (A) and (B), 250 μ m in (C).

589

590

591

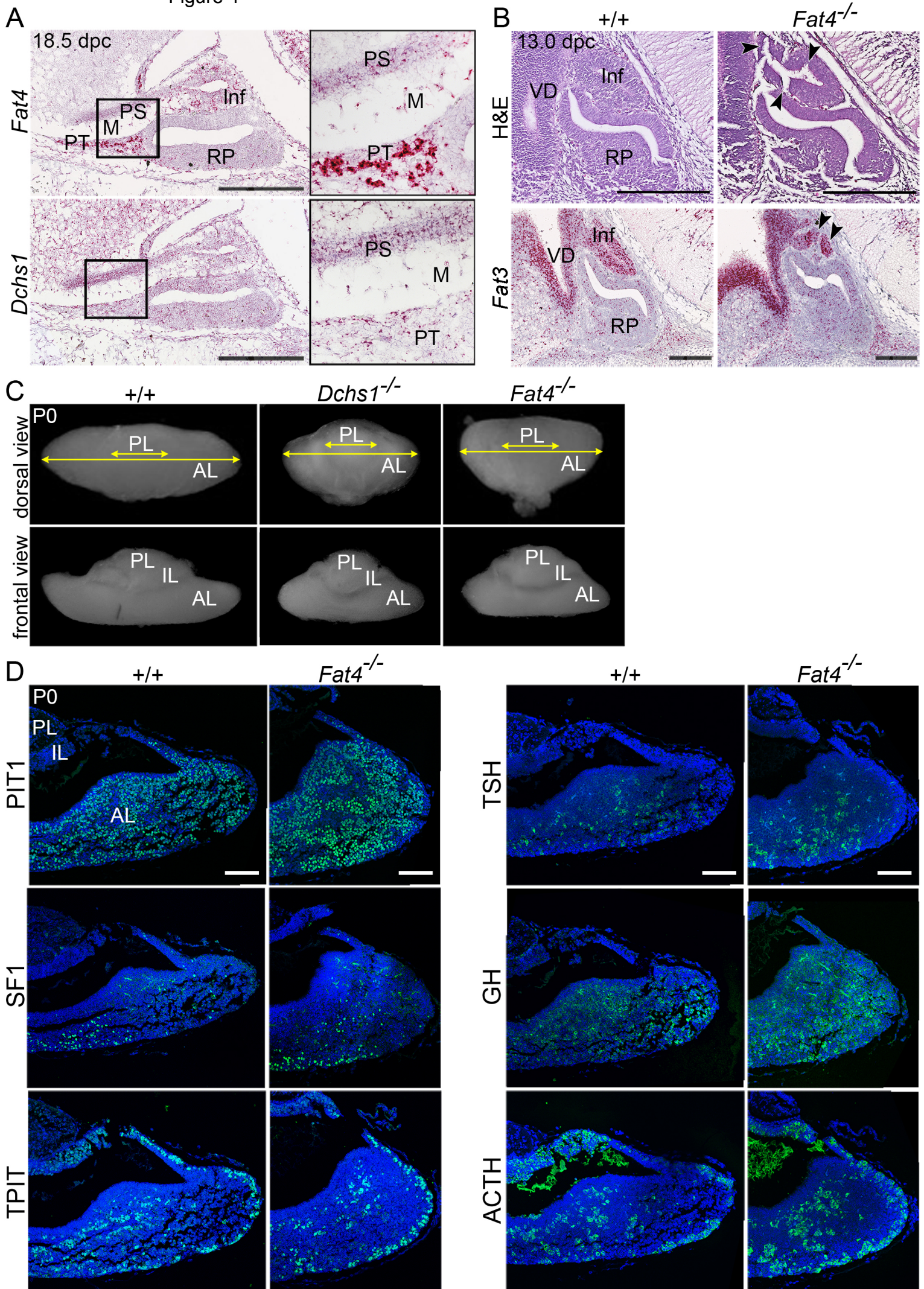


593 **Figure 4. FAT4 and DCHS1 are required for normal murine pituitary development. (A)**
594 RNAscope mRNA *in situ* hybridization on sagittal sections through wild type murine
595 pituitaries at 18.5dpc using probes against *Fat4* and *Dchs1* (n=3). Abundant *Fat4* transcripts
596 are detected in the pars tuberalis, the infundibulum, developing pituitary stalk and
597 mesenchyme surrounding definitive Rathke's pouch. Some transcripts are also detected in
598 RP. Expression of *Dchs1* is detected at low levels throughout these tissues. **(B)** Hematoxylin
599 and eosin staining of sagittal sections through *Dchs1*^{-/-} (n=5), *Fat4*^{-/-} (n=10) and control
600 pituitaries (n=15) at 13.0dpc showing invaginations in the infundibulum of *Fat4*^{-/-} mutants
601 (arrowheads), not observed in control or *Dchs1*^{-/-} embryos. RNAscope mRNA *in situ*
602 hybridization on sagittal sections through control wild type and *Fat4*^{-/-} pituitaries at 13.5dpc
603 using specific probes against *Fat3* marking the ventral diencephalon and infundibulum,
604 which is abnormal in mutants (arrowheads). **(C)** Wholemount images taken at dorsal (top
605 panels) and frontal views (bottom panel) of control, *Dchs1*^{-/-} (n=10) and *Fat4*^{-/-} (n=8)
606 pituitaries at P0. Both *Dchs1*^{-/-} and *Fat4*^{-/-} mutants have a shortened medio-lateral axis
607 affecting the anterior lobe compared to control. **(D)** Immunofluorescence staining on *Fat4*^{-/-}
608 pituitaries and littermate controls at 18.5dpc using antibodies against lineage-committed
609 progenitor markers PIT1, TPIT and SF1 and hormones TSH, GH and ACTH (n=3). Staining is
610 comparable for all markers between genotypes. Inf: infundibulum, PS: pituitary stalk, PT:
611 pars tuberalis, RP: Rathke's pouch, M: mesenchyme, VD: ventral diencephalon, PL: posterior
612 lobe, IL: intermediate lobe, AL: anterior lobe. Scale bars: 250µm in (A) and (B), 100µm in (D).

613

614

Figure 4



TABLES

Table 1. Mutations/variatioins of *FAT/DCHS* identified in patients with EPP

Patient Code	Gene	Functional Type	Func. refGene	SNP Effect	Functional Class	Codon Change	Amino Acid Change	Frequency in the Genome Aggregation Database	CADD score
D190	<i>DCHS2</i>	HIGH	exonic	NONSENSE	STOP GAINED	Cga/Tga	p.Arg1343Ter	0.135% rs150179829	38
D041	<i>FAT2</i>	LOW	exonic	SILENT	SYNONYMOUS	ttC/ttT	p.Phe1497=	0.00119% rs1024234841	11.57
D965	<i>DCHS2</i>	HIGH	exonic	NONSENSE	FRAMESHIFT	aaa/aG-	p.Lys279Serfs*10	0.00%	Not available
D965	<i>FAT2</i>	HIGH	exonic	NONSENSE	STOP GAINED	Cga/Tga	p.Arg3476Ter	0.000398% rs377026428	55
D140	<i>DCHS2</i>	MODERATE	exonic	MISSENSE	NONSYNONYMOUS CODING	aCa/aAa	p.Thr1328Lys	0.00%	27.5
D831	<i>FAT2</i>	MODERATE	exonic	MISSENSE	NONSYNONYMOUS CODING	cGc/cAc	p.Arg1250His	0.00168% rs145224294	34
D205	<i>FAT2</i>	MODERATE	exonic	MISSENSE	NONSYNONYMOUS CODING	Gat/Cat	p.Asp2720His	0.00%	23.4

Table 2. Clinical data and pituitary height of patients with variants in *FAT2* and/or *DCHS2*

Patient code	Sex	Age at the time of study (yrs)	Weight at the time of study (kg)	Height at the time of study (cm)	Endocrine disorders	Other findings	Pituitary height (mm)	Normal mean pituitary height (mm \pm SD) for age ¹
D190	Male	20.6	N/A	N/A	GHD, TSHD, ACTHD,	micropenis, cryptorchidism	2	5.63 \pm 1.00
D041	Male	16.4	59.7	162.9	GHD	NR	4	5.10 \pm 1.17
D965	Male	13.9	55	165	GHD	NR	4	5.10 \pm 1.17
D140	Female	20.7	45.2	155	GHD	NR	4	6.48 \pm 0.95
D831	Male	15.1	46	159.8	GHD, TSHD, partial ACTHD	NR	3	5.10 \pm 1.17
D205	Male	14.6	54.7	161.8	GHD, TSHD	micropenis, cryptorchidism	4	5.10 \pm 1.17

¹Tsunoda et al, Am J Neuroradiol 1997; 18:551–554

GHD: Growth hormone deficiency, TSHD: Thyrotropin hormone deficiency, ACTHD: Adrenocorticotropin hormone deficiency, NR: none reported, N/A: not available.